HEAT TRANSFER BETWEEN A PLANE SURFACE AND A PULSATING, PERPENDICULARLY IMPINGING AIR JET

by

LOUIS CASIMIR BURMEISTER

B. S., Kansas State University, 1957

A THESIS

submitted in partial fulfillment of the

requirements for the degree

MASTER OF SCIENCE

Department of Mechanical Engineering

KANSAS STATE UNIVERSITY
OF AGRICULTURE AND APPLIED SCIENCE

1959

TABLE OF CONTENTS

INTRODUCTION

The effect of forced convection has been observed and utilized for the transfer of heat in industrial and other applications for many years. However, the primary effort of investigators of forced convection heat transfer has been focused on steady state conditions. This area has been extensively treated both analytically and experimentally.

In recent years transient or unsteady conditions have achieved a position of more than academic interest. Technological developments such as atomic fission reactors, rocket nozzles, pulse jets and temperature sensitive instruments or automatic controls have made knowledge of these conditions a matter of practical importance.

The findings of observers and investigators have been that unsteady or transient conditions do affect the magnitude of convective heat transfer. Andreas (1) found that the heat transfer of heat exchangers could be improved by imparting to the exchanger a vibrational motion of 1 to 5 mm. amplitude and a frequency of 1500 vibrations per minute.

This observation is supported by that of Lemlich (10) who did an experimental investigation of the effect of vibration on the natural convection heat transfer from a horizontal, electrically heated nichrome wire and found that vibration from 39 to 122 cycles per second increased the heat flow and that the heat transfer coefficient increased with increasing "frequency amplitude". Boelter (4) also investigated analytically and

experimentally the effect of vibration on natural convection from a horizontally mounted, electrically heated tube and found that it was possible to increase heat transfer by imparting an oscillation to the tube. West (20) determined that heat transfer coefficients inside tubes for Reynolds Numbers of 3×10^4 to 8.5×10^4 were increased 60 to 70 per cent by the use of partially dampened pulsating flow from a reciprocating pump.

Thus, it can be seen that unsteady conditions, oscillations in particular, do have a definite effect upon both natural and forced convective heat transfer as previously stated. Generally, as the references cited above indicate, the effect of oscillations can be made to increase the convective heat transfer.

The area of immediate interest is that in which a pulsating jet impinges normally or at some other angle upon a plane surface. Milne-Thomson (12) treated the problem of the direct impact of two equal jets in steady flow which is the same problem as the direct impact of a jet in steady flow upon an infinite plane surface. He obtained the streamlines by use of complex variables and the Schwarz and Christoffel transformation. However, the work of Glauert (7) is most applicable in that he found solutions of the exact boundary layer equations for the velocity distribution for a jet of gas issuing from a long slot or a circular nozzle or orifice and impinging perpendicularly upon an infinite flat plate. He terms these two cases a plane and a radial wall jet, respectively. Additionally, sinusoidal oscillation of the infinite plate parallel to its own plane or

of the jet in a plane parallel to that of the plate were considered and the exact boundary layer equations solved by Glauert (6). Lighthill (8) undertook the solution of the case of an infinite stream executing sinusoidal oscillations without flow reversal and with the stream flowing normal to the axis of a rod. The exact boundary layer equations were solved for high and low ranges of oscillation frequencies. Unfortunately, his solution is not applicable to the area of immediate interest as stated beforehand except in the region of the stagnation point.

At this point, it will be noted that although some authors are concerned with a fluid jet impinging upon an infinite plane surface, no angle of impingement other than 90° from horizontal is considered and no pulsation of the jet flow rate is taken into account. Therefore, the subject of a fluid jet impinging on a plane surface and undergoing time dependent flow rate pulsations without flow reversal remains to be investigated.

NOMENCLATURE

A = constant; area, ft.^{2}

$\alpha = k/\rho c_p$ thermal diffusivity, ft.^{2}/hr.

B = constant

C = constant

c_p = specific heat at constant pressure Btu/lb.$_m$ °F

d = nozzle diameter, ft.

D = constant

δ = hydrodynamic boundary layer, (jet thickness), ft.

δ_t = thermal boundary layer thickness, ft.

F = force, lb_f

H = height of apparent jet origin above the plane surface, ft.

h = film coefficient of heat transfer, Btu/hr. $ft.^2$ ^oF

I = integral

II= integral

μ = dynamic viscosity, $lb._m$/hr. ft.

ω = frequency of jet pulsation, radians/hr.

φ = T-Te, ^oF

P = pressure, $lb_f/ft.^2$

Q = heat flow rate, Btu/hr.

ρ = mass density, $lb._m/ft.^3$

τ = time, hr.

T = temperature

T_w= temperature of plane surface, ^oF

T_e= temperature of environmental fluid, ^oF

t = temperature difference between jet and environmental fluid, ^oF

$\theta = T_w - T_e$, ^oF

r = radial distance from nozzle centerline, ft.

U = radial velocity, ft./hr.

U_1= maximum radial velocity in the radial wall jet, ft./hr.

U_e= environmental radial velocity, ft./hr.

y = vertical position above the plane surface, ft.

$\nu = \frac{\mu}{\rho}$, kinematic viscosity, $ft.^2$/hr.

Classical Dimensionless Groups

N_{Re} = Reynolds Number,

N_{Pr} = Prandtls Number,

N_{Nu} = Nusselts Number,

STATEMENT OF PROBLEM

A jet of air undergoing flow rate pulsations issues from a nozzle and impinges perpendicularly upon an infinite plane surface with a temperature difference existing between the air jet and the surface. This thesis has as its objective the investigation of the heat transfer between the plane surface and the pulsating, impinging air jet which will be termed a radial wall jet.

ANALYSIS

Rather than attempt a solution of the exact partial differential equations due to their complexity, integral equations will be derived which satisfy the same physical laws of conservation of mass and energy and momentum. The fluid properties are assumed constant and the flow to be incompressible. Bouyancy effects are taken to be negligible. Plane surface temperature is assumed to be spatially uniform.

Calculation of the thickness of the jet will first be undertaken because the thermal boundary layer which is of primary interest will later be shown to be dependent upon the hydrodynamic boundary layer. Application of a momentum balance

to a differential element and integration through the thickness of the hydrodynamic boundary layer leads to an expression for the net change in momentum flux through the wall jet along a radial element of differential length. In this analysis the total thickness of the jet as it flows over the plane surface is called the hydrodynamic boundary layer thickness. Equating this net change in momentum flux to the force of friction acting at the plane surface yields the following equation for the hydrodynamic boundary layer along the plane surface.

$$-\nu r \frac{\partial u}{\partial y}\Big|_{y=0} = \frac{d}{dr}\int_0^\delta r u^2 dy + \frac{d}{dr}\int_0^\delta r u dy \qquad (1)$$

This cannot be solved as it stands. However, by making a proper assumption as to the form of the velocity distribution through the thickness of the wall jet, the integrals in the preceding equation can be evaluated. In this matter there is some help available in the literature. An experimental investigation of a radial wall jet was performed by Bakke (2) and the velocity distribution through the thickness of the jet was determined as shown on Plate I. The predictions of Glauert (7) were confirmed. To approximate this velocity distribution let the ratio $\frac{u}{U}$ be taken as the polynomial $2\frac{y}{\delta} - \left(\frac{y}{\delta}\right)^3$. This is the usual polynomial form of velocity distribution for flow over a plate (5). But in the situation under consideration the velocity must rise from zero at the surface to a maximum and then fall to zero again at the hydrodynamic boundary of the jet. In order that these conditions may be fulfilled, a

EXPLANATION OF PLATE I

Radial wall jet velocity profiles

(A) Bakke's data for a low speed, turbulent, radial wall jet velocity profile with jet thickness taken to be that point at which $\frac{u}{u_1} = \frac{1}{2}$

(B) Assumed radial wall jet velocity profile with jet thickness taken to be that point at which $\frac{u}{u_1} = 0$

$$\frac{u}{u_1} = 48\left[2\frac{y}{\delta} - \left(\frac{y}{\delta}\right)^2\right]\left[1 - \frac{y}{\delta}\right]^2$$

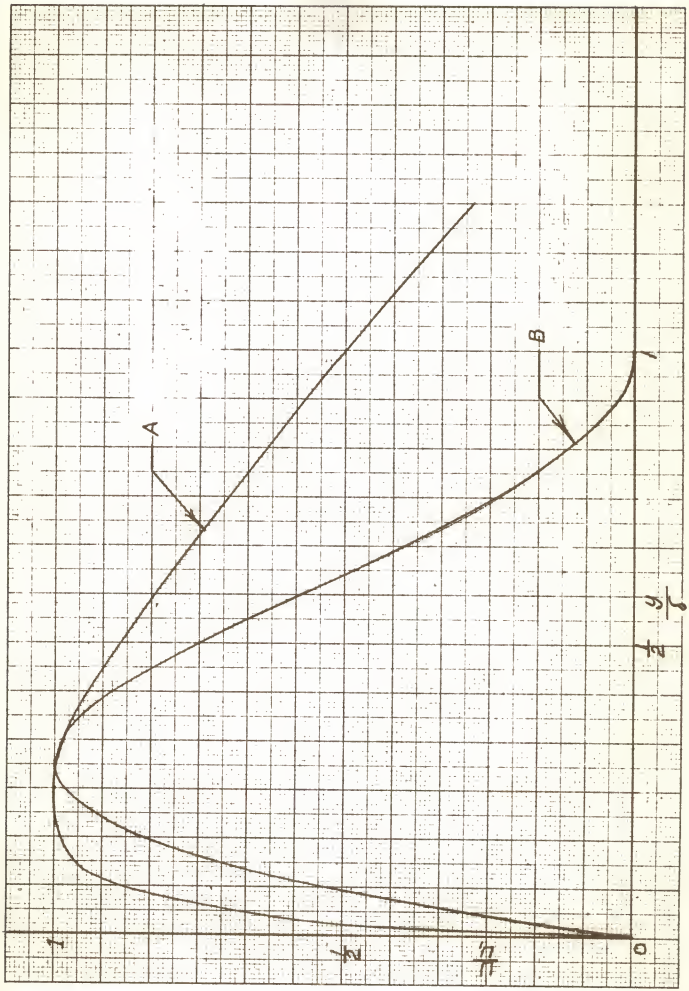
A
B
1
$\frac{1}{2}$
$\frac{y}{L}$
0
$\frac{1}{4}$
$\frac{1}{2}$
1

factor will be included so that the polynomial now appears as

$$(2)\quad \frac{u}{u_1} = 48\left[2\frac{y}{\delta} - \left(\frac{y}{\delta}\right)^2\right]\left[1-\frac{y}{\delta}\right]^n \qquad n>1$$

The exponent of the factor $1-\frac{y}{\delta}$ is arbitrary except that it must be greater than unity to insure that the slope of the velocity distribution curve will be zero at $y=\delta$. Setting n = 2 gives (3) $\frac{u}{u_1} = 48\left[2\frac{y}{\delta} - \left(\frac{y}{\delta}\right)^2\right]\left[1-\frac{y}{\delta}\right]^2$. Rewriting (1) as (4) $-\nu r \left.\frac{du}{dy}\right|_{y=0} = \frac{d}{dr}\left[u_1^2 r \int_0^\delta \left(\frac{u}{u_1}\right)^2 dy\right] + \frac{d}{dr}\left[u_1 r \int_0^\delta \frac{u}{u_1}\, dy\right]$ and substituting (3) into (4) the following is obtained after evaluation of the integrals,

$$(5)\quad -\frac{2\nu r u_1}{\delta} = \frac{8(48)^2}{315}\frac{d}{dr}\left[u_1^2 r\delta\right] + \frac{2(48)}{15}\frac{d}{dr}\left[u_1 r\delta\right]$$

Multiplying both sides by δ and taking the indicated partial derivatives and simplifying leads to

$$(6)\quad \frac{d(\delta^2)}{dr} + \frac{7}{64u_1}\frac{d(\delta^2)}{dr} = -\delta^2\left[\frac{2}{u_1^2 r}\frac{d(u_1^2 r)}{dr} + \frac{7}{32u_1^2}\frac{du_1}{dr}\right] - \frac{35\nu}{32u_1}$$

Obviously, U_1 is a variable dependent upon time and radial position from the nozzle center line. Up to this point, it has not been necessary to specify the form of the dependency, but solution of (8) requires that this now be done. Bakke (2) found that maximum radial wall jet velocity varies inversely with the radial distance from the nozzle centerline. A relationship of the form (7) $U_1 = Ar^m$ may, therefore, be assumed for steady state conditions. Substitution of this relationship into

equation (6) would permit its solution if $\frac{d(\delta^2)}{dr} = 0 = \frac{dU_1}{dr}$ signifying that a steady state hydrodynamic boundary layer is being considered. The problem is then reduced to solving the equation

$$(8) \qquad \frac{d(\delta^2)}{dr} + \delta^2\left[\frac{2}{U_1^2 r}\frac{d(U_1^2 r)}{dr}\right] = -\frac{35\nu}{512\,U_1}$$

An integrating factor for this ordinary differential equation is

$$(9) \qquad e^{2\int \frac{d(U_1^2 r)}{U_1^2 r}} = (U_1^2 r)^2$$

So, (10) $$\delta^2 = -\frac{35\nu}{512}(U_1^2 r)^{-2}\int U_1^3 r^2\, dr + C(U_1^2 r)^{-2}$$

Substituting $U_1 = Ar^m$ into (10),

$$(11) \qquad \delta^2 = -\frac{35\nu}{512}(U_1^2 r)^{-2}\int A^3 r^{3m+2}\, dr + C_1 r^{-2(1+2m)}$$

is obtained.

Evaluation of the integral in (11) yields

$$(12) \qquad \delta^2 = -\frac{35\nu}{1536A(1+m)} r^{1-m} + C_1 r^{-2(1+m)} \qquad m \neq -1$$

This, as mentioned before, is the steady state hydrodynamic boundary layer and serves as an initial condition for equation (6). The value of the exponent m is subject to some question. In the region of the stagnation point it is probably positive (5) while Bakke (2) found that at some distance from the nozzle centerline it is negative. This question is deferred until later, and treated in the section presenting experimental results under the subheading of maximum radial wall jet velocity variation along the plane surface.

Returning to the equation (6) of the unsteady hydrodynamic boundary layer it is noted that U_1 must have its dependence on time specified as well as on r as has already been done by equation (7). After some thought, it is logical to conclude that some time will be required for a change in velocity at the nozzle to make itself felt at a downstream position, r. Therefore, the expression for the dependence of U_1 on time should contain a term giving the time lag at any radial position. This time lag term is assumed to be Dr^n where D and n must be experimentally determined.

Since the governing equation (6) is linear, the principle of superposition may be applied to the phenomenon. In other words, knowledge of the hydrodynamic boundary layer's response to a step change in velocity at the nozzle would enable prediction of its response to any other form of change in nozzle exit velocity. Now, a step change in nozzle exit velocity may be expressed by (13) $U_1 = Ar^m[B \pm \Delta(\tau - Dr^n)]$ where B is a constant greater than unity to prevent flow reversal and $\Delta(\tau - Dr^n)$ is the unit step function with a time lag. Unfortunately, this specification of U_1 renders equation (6) too difficult to solve, except, perhaps, by means of a digital computer. By choosing U_1 to be of the form

(14) $U_1 = Ar^m[B + \sin(\omega\tau - Dr^n)]$

where B is as defined above and ω is the frequency of velocity oscillation or pulsation, equation (6) is more amenable to

classical methods of solution. Form (14) is one of the most likely forms of nozzle velocity pulsation and, additionally, any form of velocity pulsation should be able to be synthesized by a Fourier Series of sines and the response to it calculated through knowledge of the hydrodynamic boundary layer's response to form (14).

Writing the subsidiary equations to (8) which is a Lagrange equation, the relations below are achieved

$$(17)\quad \frac{dr}{1} = \frac{d\tau}{\frac{7}{64\mu_1}} = \frac{d(\delta^2)}{-\delta^2\left[\frac{2}{\mu_1^2 r}\frac{d(\mu_1^2 r)}{dr} + \frac{7}{32\mu_1^2}\frac{d\mu_1}{d\tau}\right] - \frac{35\nu}{512\mu_1}}$$

Substituting (16) into (17) and taking the indicated partial derivatives leads to

$$(18)\quad \frac{dr}{1} = \frac{d\tau}{\frac{7}{64Ar^m[B+\sin(\omega\tau-Dr^n)]}} =$$

$$\frac{d(\delta^2)}{-\delta^2\left\{\frac{2(1+2m)}{r} - \frac{4nDr^{n-1}\cos(\omega\tau-Dr^n)}{B+\sin(\omega\tau-Dr^n)} + \frac{7\omega\cos(\omega\tau-Dr^n)}{32Ar^m[B+\sin(\omega\tau-Dr^n)]^2}\right\} - \frac{35\nu}{512Ar^m[B+\sin(\omega\tau-Dr^n)]}}$$

The complete integral of (6) may be obtained by the evaluation of any two of the three relations given above. Evaluation of the above relations also enables the hydrodynamic boundary layer to be solved for by means of the method of characteristics.

Consider first

$$(19)\quad dr = \frac{d\tau}{64Ar^m[B+\sin(\omega\tau-Dr^n)]}$$

Rearranging,

$$(20)\quad \frac{d(Dr^{1-m})}{d\tau} - \frac{64}{7}AD(1-m)[B+\sin(\omega\tau-Dr^n)] = 0$$

Realizing that the term Dr^n represents the time required for a change in nozzle exit velocity to reach a downstream radial position, it can be seen that knowledge of a possible relation between m and n would simplify (20). Since $U = dr/d\tau$, (7) can be substituted for U and the simple differential equation $Ar^m = dr/d\tau$ results. Evidently, $\tau_2 - \tau_1 = r^{1-m}/A(1-m)$. This indicates that the exponent n can be said to be 1-m. Putting $n = 1-m$ into (20) and letting $z = \omega\tau - Dr^{1-m}$, yields

$$(21)\quad \frac{dz}{d\tau} - \omega + \frac{64}{7}AD(1-m)[B+\sin(z)] = 0$$

which can be solved by separation of variables as follows:

$$(22)\quad \int \frac{dz}{b+c\sin(z)} = \tau + C_3$$

$$(23)\quad \frac{-2}{\sqrt{b^2-c^2}}\tan^{-1}\left[\sqrt{\frac{b-c}{b+c}}\tan\left(\frac{\pi}{4}-\frac{z}{2}\right)\right] = \tau + C_3 \qquad b^2 > c^2$$

$$(24)\quad \frac{-1}{\sqrt{c^2-b^2}}\ln\left[\frac{c+b\sin(z)+\sqrt{c^2-b^2}\cos(z)}{b+c\sin(z)}\right] \qquad c^2 > b^2$$
$$= \tau + C_3$$

$$(25)\quad \mp\frac{1}{b}\tan\left(\frac{\pi}{4}\mp\frac{z}{2}\right) = \tau + C_3 \qquad b = \pm c$$

Now, $b = \omega - \frac{64}{7} ABD(1-m)$ and $c = -\frac{64}{7} AD(1-m)$

For $b = \pm c$, $\omega = \frac{64}{7} AD(1-m)(B \mp 1)$

Since $\omega \geq 0$ and $B \geq 1$, this case may be possible. A like argument for the remaining two cases shows that equation (24) is also possible. However, the case for which $b^2 > c^2$ most easily illustrates the difficulties to follow. Thus,

$$(26) \quad \tan\left(\frac{\pi}{4} - \frac{z}{2}\right) = \sqrt{\frac{b+c}{b-c}} \tan\left[-\frac{1}{2}\sqrt{b^2-c^2}\,(\tau + c_3)\right]$$

Now,

$$(27) \quad \frac{b+c}{b-c} = \frac{\omega - \frac{64}{7} AD(1-m)(B+1)}{\omega - \frac{64}{7} AD(1-m)(B-1)}$$

Note that (B + 1) is the upper limit of the maximum velocity variation while (B - 1) is the lower limit. If $B \gg 1$,

$$\frac{b+c}{b-c} \simeq 1$$

implying a relatively small flow rate pulsation. In this case

$$(30) \quad Dr^{1-m} = \frac{64}{7} ABD(1-m)\tau - \left[\frac{\pi}{2} + c_3\left(\omega - \frac{64}{7} ABD(1-m)\right)\right]$$

This solution is one of the two independent integrals of the subsidiary equations required to form the general integral of equation (8) for a sinusoidal flow rate pulsation at the nozzle. Another independent integral can be found from the subsidiary equations by evaluating with n = 1-m the relation from equation (18)

$$(31)\quad \frac{d\tau}{\frac{7}{64Ar^m[B+\sin(z)]}} = \frac{d(\delta^2)}{-\delta^2\left\{\frac{2(1+2m)}{r} - \frac{4mDr^{m-1}\cos(z)}{B+\sin(z)} + \frac{7\omega\cos(z)}{32Ar^m[B+\sin z]}\right\}} - \frac{35\nu}{512Ar^m[B+\sin(z)]}$$

Substituting from equation (30) and simplifying,

$$(32)\quad \frac{d(\delta^2)}{d\tau} + \frac{64}{7}\delta^2\left\{\frac{2AD(1+2m)[B+\cos(\omega-\frac{64}{7}ABD(1-m))(\tau+c_5)]}{\frac{64}{7}ABD(1-m)\tau-[\frac{\pi}{2}+c_5(\omega-\frac{64}{7}ABD(1-m))]} - 4AD(1-m)\sin[(\omega-\frac{64}{7}ABD(1-m))(\tau+c_5)] + \frac{7\omega\sin[(\omega-\frac{64}{7}ABD(1-m))(\tau+c_5)]}{32[B+\cos(\omega-\frac{64}{7}ABD(1-m))(\tau+c_5)]}\right\} = -\frac{5}{8}\nu$$

In order to solve this ordinary differential equation, an integrating factor must be found. This integrating factor could be obtained from $e^{\int\{\}\,d\tau}$. The quantity enclosed in the braces of equation (32) can possibly be integrated with respect to τ. But the next step which involves integrating $-\frac{5}{8}\nu\int e^{\int\{\}\,d\tau}\,d\tau$ would be extremely difficult except by numerical means even with the assumed relatively small flow rate pulsation. The thermal boundary layer is next shown to depend upon the above integral. A vast increase in difficulty of the resultant equations then becomes evident.

The thermal boundary layer will not be dealt with in detail here, but the governing partial differential equation derived in Appendix III is merely rewritten. This equation is

(34) $$\frac{4\alpha}{\delta_t} = \frac{128}{5r}\frac{d\left(\frac{u_1 r}{\delta}\right)}{dr}\delta_t^2 + \frac{256}{5}\frac{u_1}{\delta}\delta_t\frac{d\delta_t}{dr} + \frac{d\delta_t}{d\tau}$$

If $\frac{d\delta_t}{d\tau} = 0$ which implies no flow pulsation and constant plane surface and jet temperatures equation (35) results with rearrangement,

(35) $$\frac{d(\delta_t^3)}{dr} + \frac{3\delta}{2(u_1 r)}\frac{d\left(\frac{u_1 r}{\delta}\right)}{dr}\delta_t^3 = \frac{15\delta}{64 u_1}\alpha$$

An integrating factor is (36) $$e^{\frac{3}{2}\int\frac{\delta}{u_1 r}\,d\left(\frac{u_1 r}{\delta}\right)} = \left(\frac{u_1 r}{\delta}\right)^{3/2}$$

Thus, (37) $$\delta_t^3 = \frac{15\alpha}{64}\left(\frac{u_1 r}{\delta}\right)^{-\frac{3}{2}}\int\left(\frac{u_1 r}{\delta}\right)^{\frac{3}{2}}\frac{\delta}{u_1}\,dr + C_2\left(\frac{u_1 r}{\delta}\right)^{-\frac{3}{2}}$$

Now δ^2 was previously found to be given by equation (10) for steady flow conditions. Since $u_1 = Ar^m$,

$$(38)\quad \frac{\delta}{\mu_1 r} = \sqrt{\frac{-35\nu}{1536A^3(1+m)}\, r^{-(1+3m)} + \frac{C_1}{A^2}\, r^{-2(2+3m)}}$$

So equation (37) takes the form

$$(39)\quad \delta_t^3 = \frac{15\alpha}{64}\left(\frac{\mu_1 r}{\delta}\right)^{-\frac{3}{2}} \int \frac{r\,dr}{\left[\frac{-35\nu}{1536A^3(1+m)}\, r^{-(1+3m)} + \frac{C_1}{A^2}\, r^{-2(2+3m)}\right]^{\frac{1}{4}}} + C_3 r^{\frac{-3(1+3m)}{4}}$$

At this point a choice is available if the above integral is to be evaluated. Either m can be specified or C_1 can be set equal to zero. Let $C_1 = 0$. When this is done it is found that

$$(40)\quad \delta_t^3 = \frac{5\alpha}{16(3+m)}\left[\frac{-35\nu}{1536A^3(1+m)}\right]^{\frac{1}{2}} r^{\frac{3(1-m)}{2}} + C_3 r^{\frac{-3(1+3m)}{4}}$$

The ratio of $\frac{\delta_t}{\delta}$ is then

$$(41)\quad \frac{\delta_t}{\delta} = \sqrt[3]{-\frac{96}{7}\left(\frac{1+m}{3+m}\right)\frac{1}{P_r} + C_4 r^{\frac{-3(3+m)}{4}}} \qquad m \neq -1$$

To determine C_4 the plane surface is assumed to be unheated until $r = r_o$. Then

$$(42)\quad \frac{\delta_t}{\delta} = \frac{1}{\sqrt[3]{\frac{7}{96}P_r}} \sqrt[3]{-\left(\frac{1+m}{3+m}\right)\left\{1-\left[\frac{r_o}{r}\right]^{\frac{3(3+m)}{4}}\right\}} \qquad m \neq -1$$

which compares favorably with the solution obtained by Eckert and Drake (5) for flow of an infinite stream parallel to a heated plate demonstrating the validity of the method used in this thesis. Also, equation (42) can be used as an initial condition for equation (34).

The ratio $\frac{U_1}{\delta}$ occurs frequently. Previously the difficulty of calculating δ was illustrated and recourse to numerical methods was shown to be necessary. Reliance upon numerical solutions for determination of the thermal boundary layer thickness is obviously even more inevitable. The many calculations required for solution of the thermal boundary layer thickness in particular, make programming of these equations on a digital computer mandatory.

Once the thermal and hydrodynamic boundary layer thickness are known, the film coefficient of heat transfer can be computed. Computation would be as given below. The heat transferred by convection per unit area, Q, is given by

$$(43) \quad Q = h\left(T_{surface} - T_{jet}\right)$$

This heat must leave the plane surface by conduction through the gas layer adjacent to the plane surface. So,

$$(44) \quad Q = -k \left.\frac{\partial T_{jet}}{\partial y}\right|_{y=0}$$

Equating these two expressions for Q produces

$$(45) \quad h = -\frac{k}{T_{surface} - T_{jet}} \left.\frac{\partial T_{jet}}{\partial y}\right|_{y=0}$$

If $T_{jet} = T_{environment}$

$$(46) \quad h = \frac{k}{\theta} \left.\frac{\partial \theta}{\partial y}\right|_{y=0} = k \left.\frac{\partial\left(\frac{\theta}{\theta}\right)}{\partial y}\right|_{y=0} = \frac{3k}{2\delta_t}$$

The thermal boundary layer thickness, δ_t, being known thus enables h to be determined.

This analysis is intended to show that the feasibility of solving the partial differential equations derived in Appendix II and III governing the thermal and hydrodynamic boundary layer thicknesses is slight unless numerical methods are used. A digital computer is suggested as the best tool to facilitate a numerical method of solution.

DESCRIPTION OF EQUIPMENT

An experimental study of the problem to check any result of the mathematical analysis and to gain knowledge of the radial wall jet's heat transfer and kinetic characteristics was undertaken.

Air for the jet was supplied by a centrifugal fan driven by a variable speed motor in the range of 0-1800 rpm. Air was delivered from the fan to the experimental apparatus from the fan outlet duct through a 36 foot length of 1/4 inch i.d. rubber hose which also served to damp out pulsations in the air flow rate delivered by the fan. A picture of this centifugal fan is shown in Plate II.

The experimental apparatus itself is shown in Plate III. The rubber hose through which air flowed from the centrifugal fan was screwed into a series of 3/4" pipe fittings connected by means of a reducer to an expansion chamber constructed of a 6" length of 1½" pipe. In the uppermost fitting, a 3/4" tee one foot above the nozzle screwed into the bottom of the expansion chamber, a thermocouple was inserted for measurement of the jet

air temperature before impingement. The second 3/4" tee, immediately atop the expansion chamber, provided an outlet controlled by a solenoid valve in series with a gate valve for variable resistance to flow for variation of flow pulsation amplitude. A relay operated by the output of a sinusoidal function generator allowed the solenoid valve to be opened and closed with a frequency of 0.02-20 cps while producing a square waveform of flow rate pulsation.

Two pressure taps, diametrically opposed, were provided in the expansion chamber for determination of the pressure drop across the nozzle. One tap 3 1/2" above the nozzle led to a Meriam water micromanometer. Into the other tap, 1 1/4" above the nozzle was screwed a Consolidated Electrodynamics, 0-10psig, pressure transducer. The output of this transducer was recorded on a one-channel Sanbourn recorder to give a record of the pressure drop across the nozzle which determines the jet flow rate.

Nozzles from which the jet of air issued were calibrated for volumetric flow rate (CFH) versus pressure drop across the nozzle (in. H_2O). Calibrated nozzles were available in 1/8", 1/4", 1/2", 3/4", 1", and 1 1/4" diameters. Nozzle design is shown in Plate IV.

The plane surface upon which the air jet impinged was realized by a 2 feet square of asbestos board 1/8" thick screwed to the top of a cubic wooden box 2 feet on a side. In the center of the asbestos board and with the two upper surfaces flush, were located a 4½" diameter copper disk 1/4" thick and a copper

EXPLANATION OF PLATE II

View of the centrifugal fan


C-50590-B

EXPLANATION OF PLATE III

Closeup of expansion chamber assembly

PLATE III

EXPLANATION OF PLATE IV

Design of nozzles used.

Nozzle diameter (d) = 1/8", 1/4", 1/2", 3/4", 1", & 1 1/4"

PLATE IV

A & B Are
Parallel Within 0.005
0.378
0.375
5/8
1/4
3/32
13/32
1/64
3/16
30°
A
B
d
45° Chamfer From
1 13/32 - 1 1/2 - 16UNC - 2A
1 5/8
Scale: Double
Material: Aluminum

annulus of the same thickness called the guard ring which had an outer diameter of 8½" and an inner diameter of 4 5/8". A 1/16" air gap existed between disk and guard ring. Plate V shows this equipment.

Heating of the central disk was accomplished through the use of a coiled electrical heating element on a ceramic mounting separating the disk from the current carrying resistance wire. The guard ring was heated in a similar manner. All heaters were controlled by Variacs and the rate of energy dissipation read from wattmeters. The cavity of the box was filled with glass wool insulation so that heat loss from the back of the central disk could be counted as negligible. In order that the heat given to the central disk by its heater be transferred only to the air jet, the outer circumference of the disk and inner circumference of the guard ring were maintained as nearly as possible at the same temperature.

Equality of disk and guard rim temperatures was attained by the use of four pairs of copper-constantan thermocouples equally spaced along the common circumference. One thermocouple of each pair was mounted in a grove on the rim of the central disk so that the hot junction comprised the entire thickness of the disk. The other thermocouple of each pair was mounted directly opposite the disk rim thermocouple in a similar fashion.

Upper surface temperatures of the disk were measured by means of ten copper-constantan thermocouples inserted as shown

EXPLANATION OF PLATE V

View of equipment reading from left to right:

One-channel Sanborn recorder
Meriam water micromonometer
Expansion chamber and heated box assemblies
Switching box
Thermos bottle for thermocouple cold junction
Wattmeter for central disk
Square-wave function generator
Electronic null-balance indicator
Speed-O-Max twenty point recorder

PLATE V

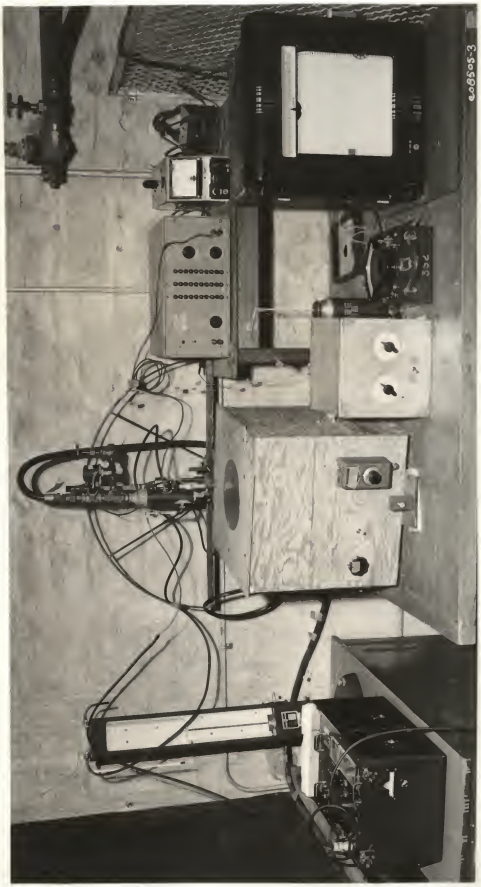

on Plate VI and their voltage output determined by a potentiometer when steady state conditions prevailed. Standard calibration tables were used to determine indicated temperatures. When the jet flow rate pulsated, the thermocouple output was recorded on a Speed-O-Max twenty point recorder. All thermocouple cold junctions were maintained at 32°F by immersion in an ice bath.

The expansion chamber assembly and heated disk assembly were mounted in a frame which permitted the nozzle centerline to intersect the center of the central disk's upper surface. Also, the height of the nozzle above the central disk and the angle of impingement could be varied. This arrangement is indicated in Plate VII.

A hot wire anemometer was used to determine maximum velocity variations of the radial wall jet. For this phase of the experimental investigation a 2 feet diameter glass mirror was used on which a radial line divided into 1/16ths of an inch was drawn in ink. The hot wire probe was held in a dissecting microscope stand to give controlled vertical movement. This stand traveled along runners for radial positioning of the hot wire. By tilting the barrel of the dissecting microscope stand it was possible to place the hot wire more nearly in the stagnation region of the air jet. For measurement of velocities while the jet was pulsing the voltage across the hot wire while the anemometer was operated as a constant current device could have been recorded on a two channel Sanborn recorder. Simultaneous recording of this voltage and pressure at the expansion chamber would

EXPLANATION OF PLATE VI

Detail of thermocouple installation in copper disk and annulus. The thermocouple hot junction was bent at 90° and placed in a groove on the upper surface. It was then soldered in place and the upper surface polished flat.

PLATE VI

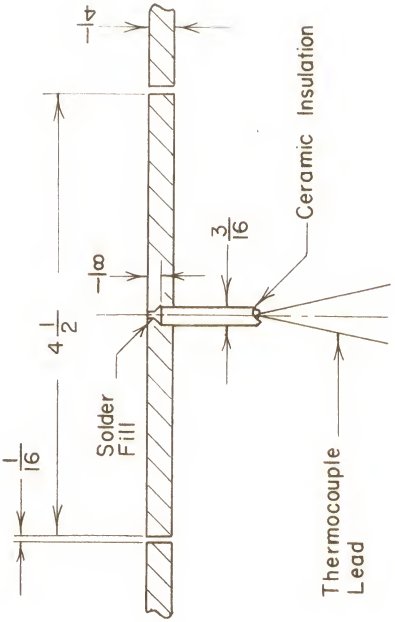
1/4
Ceramic Insulation
3/16
1/8
4 1/2
Solder Fill
1/16
Thermocouple Lead

EXPLANATION OF PLATE VII

View of expansion chamber assembly and heated disk assembly mounted for variable impingement angle and nozzle elevation.

PLATE VII

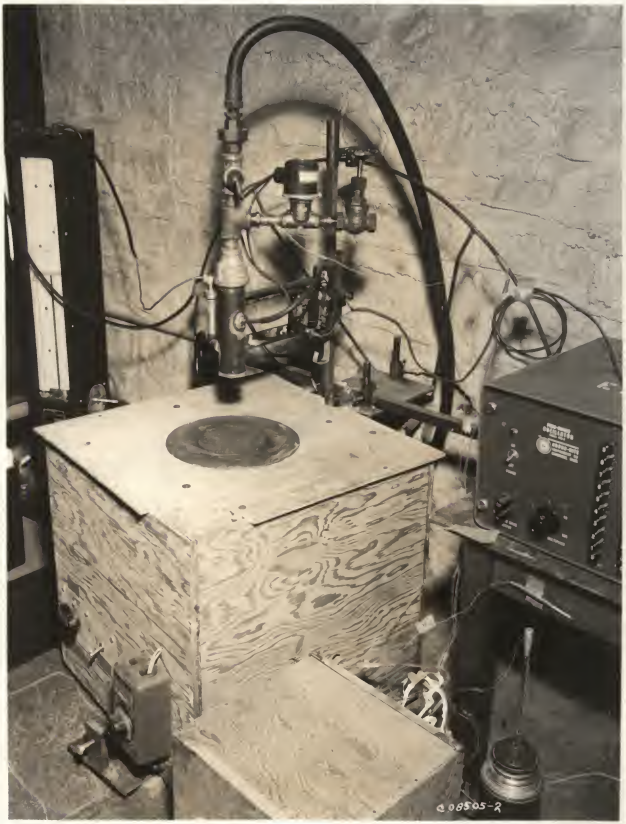

have enabled variations of velocity at any radial position to be compared to the exit velocity at the nozzle. Plate VIII shows this arrangement of equipment.

EXPERIMENTAL RESULTS

To correlate experimental data, a dimensional analysis was performed on the variables thought to determine the film coefficient of heat transfer. This analysis is presented in Appendix III. Conventional dimensionless groups such as Reynolds, Prandtls, and Nusselts numbers were obtained. In addition, since pulsating flow was considered, dimensionless groups involving the frequency and amplitude of pulsations were derived. The Reynolds number at the nozzle was restricted to the range of $1.8 \times 10^{3+0}$ to 4.8×10^{3}.

Influence of Reynolds Number

Perry (14) did experimental work with a heated jet impinging at various angles upon a plane surface and evaluated the dependence of Nussults number upon Reynolds number. He found that for perpendicular impingement Nusselts number varied as the 0.7 power of Reynolds number. His work, however, was conducted with air jets issuing from nozzles and heated to temperatures in the range of 1,112°F and with Reynolds numbers at the nozzle ranging from 7×10^{3} to 3×10^{4}. It was not felt that this dependence of Nusselts upon Reynolds number could be taken as valid for the case treated in this thesis without first checking

EXPLANATION OF PLATE VIII

View of equipment and its arrangement for measurement of velocities.

PLATE VIII

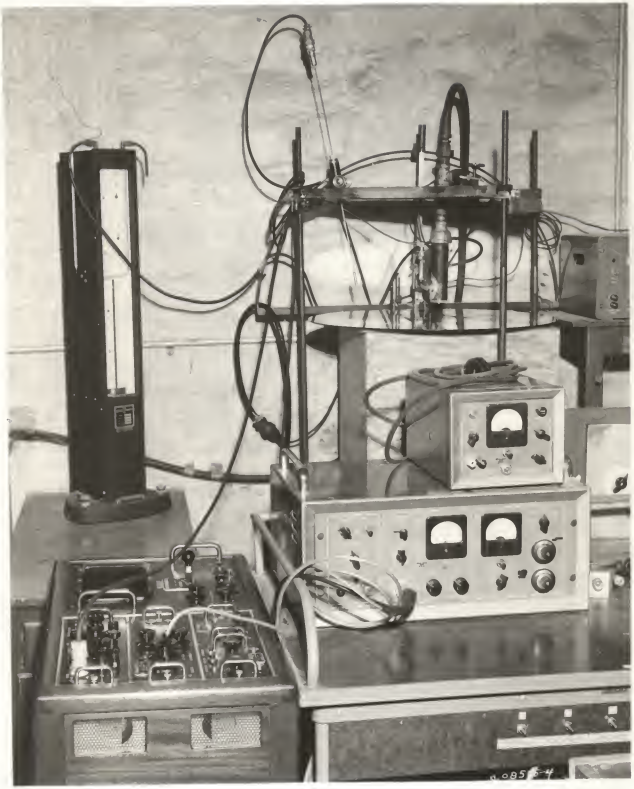

by independent experimental data the value of the exponent of Reynolds number. The investigation was confined to jets issuing in steady flow from 1/4" diameter nozzle and with Reynolds numbers in the range of 1.8×10^3 to 4.8×10^3 with the average plane surface temperature restricted to 147 to 310°F.

The experimental procedure is given so that the validity of the work may be judged. The disk and guard ring heaters were turned on and these surfaces allowed to come to thermal equilibrium with their surroundings. Heaters were adjusted to make the temperature of the inner guard ring rim equal to that of the outer disk rim. Time required for these conditions of equilibrium to be attained was generally about four hours during the initial start-up period. After changing the jet flow rate from its value for the first run of data, about two hours elapsed before steady state conditions once more prevailed. Temperatures were read at intervals during periods of warmup or flowrate change to determine the occurance of steady state conditions as evidenced by unchanging temperatures. Data as presented in Table I was then recorded which consumed approximately twenty minutes. Six runs were taken at a ratio of $H/d = 7.16$, four runs at $H/d = 15.2$, and four runs at $H/d = 43.7$.

Heat input to the central disk as read from a wattmeter was then corrected for radiation to the room and for radial heat transfer to the guard ring. The last correction was necessitated by the fact that it was rarely ever possible to exactly equalize guard ring and disk rim temperatures. Heat transfer

to or from the disk in this manner was negligible due to the low thermal conductivity of the air gap between the guard ring and disk -- roughly, $0.0938(T_{guard}-T_{disk})$Btu/hr. Calculation of the radiant heat transfer from the disk to the room proved to be the most troublesome and the largest source of possible error. During installation of the thermocouples the copper disk was polished. Its emissivity was then approximately 0.04. In spite of preliminary heating, the disk surface was found to be incompletely oxidized before data were recorded. Emissivity, therefore, underwent a gradual increase while data were taken to the value of 0.8 at the conclusion of data taking.

The seriousness of this change in disk emissivity is shown by the following illustration: at an average disk temperature of 251°F and a disk heater output of 434.0 Btu/hr. radiant heat transmission from disk to room was 1.22 and 24.4 Btu/hr. at disk emissivities of 0.04 and 0.8, respectively. This means that radiation could account for 0.28 to 5.6 per cent of the disk heater output. Oxidation of the copper disk, fortunately, occurred very slowly so that a gradual increase of emissivity was compensated for by slowly increasing the emissivity used in calculating radiant heat transfer. Error introduced by such a procedure is estimated not to exceed 3 per cent. Temperatures were recorded with an estimated accuracy of 0.2°F and the upper surface area of the central disk was known with an accuracy of four significant figures.

Calculation of the film coefficient of heat transfer between the plane surface represented by the central disk and the radial wall jet was done by substituting data into the equation $Q = hA(T_{disk} - T_{jet})$ where:

Q = heat transferred between disk and radial wall jet, Btu/hr.

A = area of disk, $ft.^2$

T_{disk} = arithmetic average disk temperature, ^oF

T_{jet} = jet temperature before impingement, ^oF

and solving for h. Correlated data taken from Table I for this phase of the investigation is shown on Plate IX. The value of the exponent of Reynolds number was determined to be 0.66 ± 3 per cent with all fluid properties taken at the arithmetic average of mean disk temperature and jet fluid temperature before impingement.

Influence of H/d Ratio

The height of the apparent jet origin above the plane surface was felt to affect the value of the film coefficient and so was included in the list of variables upon which the dimensional analysis was performed. According to this analysis, the ratio of the height of the apparent jet origin above the plane surface to the nozzle diameter was the dimensionless group involved.

Determination of the value of the exponent of H/d was achieved with the data that had been gathered for the evaluation of the influence of Reynolds number upon the film coefficient of heat transfer. For this reason, a recounting of experimental

EXPLANATION OF PLATE IX

Nusselts (hH/k) number vs. Reynolds number (Vd/ν) for a steady air jet impinging perpendicularly upon a heated disk from data of Table I.

□ H/d = 7.16

⊙ H/d = 15.2

△ H/d = 43.7

Slope of the curves is 0.66 ± 3 per cent.

$Nu \times 10^{-2}$
$Re \times 10^{-3}$

procedure and sources of possible error is not undertaken here. It is only noted again that the probable error of the immediately following result is ± 3 per cent. Plotting Nusselts number versus H/d for Reynolds numbers of 2×10^3, 3×10^3, and 5×10^3 indicated that Nusselts number varies as the +0.76 power of H/d. The range of the existent data could not have been extended much beyond 43.7 due to limitations in the travel of the nozzle support assembly without use of a smaller nozzle than the 1/4" diameter mainly used. It is recognized that lower ratios than the present minimum of 7.16 would have been possible. But, although, only three values of H/D were used, a straight line fitted the data so well that it was not thought necessary to gather data for other values of H/d. Plate X illustrates the correlation of data taken from Table I for this phase of the investigation.

Influence of a/V Ratio

Previous investigators such as Lemlich (10) and Boelter (4) discovered that the amplitude with which a horizontal, electrically heated tube was vibrated had an influence upon the magnitude of natural convective heat transfer. Lighthill (11) concurs for sinusoidally pulsating flow without flow reversal normal to a tube. Amplitude of flow pulsation was therefore placed among the list of variables to be included in the dimensional analysis of Appendix I and the ratio of amplitude of velocity pulsation to the mean nozzle exit velocity was found to be the

EXPLANATION OF PLATE X

Nusselts number (hH/k) versus H/d for a steady air jet impinging perpendicularly upon a heated disk from data of Table I.

□ $R_e = 2 \times 10^3$

⊙ $R_e = 3.5 \times 10^3$

△ $R_e = 5 \times 10^3$

Slope of the curves is 0.75.

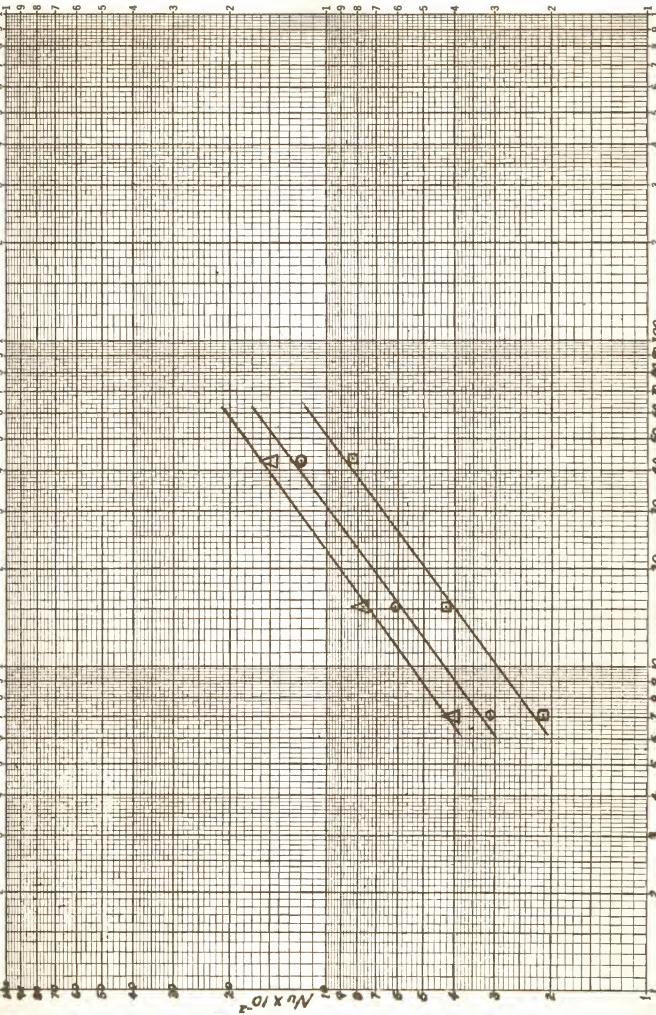
$Nu \times 10^{-3}$
$\frac{P}{H}$
A
B
C
D
E

TABLE I

Pulsation amplitude	Pulsation frequency	Nozzle elevation	Nozzle diameter	Mean Nozzle velocity	Wattmeter reading	Jet temp.	Disk average temp.	Guard ring minus disk rim temperature
ft/sec.	cps	in.	in.	ft/sec.	watts	°F	°F	°F
0	0	1.0	0.25	29.4	159.3	90.8	242.7	0.63
0	0	1.0	0.25	21.1	164.8	101.6	310	-1.7
0	0	1.0	0.25	21.1	124.4	98.3	251	2.1
0	0	1.0	0.25	21.1	123.3	98.8	242.1	0.8
0	0	1.0	0.25	37.5	162.8	93.5	225	-0.9
0	0	1.0	0.25	47.2	144.4	90.6	203.3	-0.23
0	0	3.0	0.25	22.8	66.75	90	168.6	0.6
0	0	3.0	0.25	28.4	73.8	91.8	168	-0.4
0	0	3.0	0.25	38.2	102.6	89.8	177.9	0.13
0	0	3.0	0.25	47.2	130	88.6	188.4	0.8
0	0	10.13	0.25	19.6	43.2	94.4	173.6	-0.93
0	0	10.13	0.25	37.4	105	91.2	226	-0.67
0	0	10.13	0.25	28.6	44.1	91.4	155.6	0.33
0	0	10.13	0.25	44.9	46.8	92.8	147.3	-0.97
0	0	1.50	0.125	55.4	72.4	93.6	169.9	-2.1
0	0	6.0	0.50	12.2	74.21	91.5	195.5	-0.9

dimensionless group whose exponent must be determined.

The procedure for taking data was the same as that given in the section describing the influence of Reynolds number upon Nusselts number. The exceptions to this procedure were that a square wave form of flow rate pulsation was maintained at a frequency of 2 cps. with a constant mean flow rate at the nozzle exit. Amplitude at the nozzle varied from 9.73 per cent to 31.5 per cent of the mean flow velocity at the nozzle. Data from which the curve of Plate XI was drawn is presented in Table II. Observation of this curve reveals that a plot of Nasselts number versus a/V indicates no dependence of Nusselts number upon the ratio a/V for the conditions studied. Reynolds number at the nozzle was constant at $2 \times 10^3 \pm 3$ per cent.

Influence of $\omega d/V$

Since the subject of pulsating jets was the topic of study of this thesis, the effect of pulsation frequency upon the film coefficient of heat transfer between the radial wall jet and the plane surface was a natural question to treat experimentally. The dimensional analysis of Appendix I yielded the ratio of pulsation frequency times nozzle diameter to the mean nozzle exit velocity as the dimensionless group with which to correlate experimental data.

Data taking procedure was unvaried from that described in the previous sections except that all factors other than pulsation frequency were held constant. The ratio of H/d equalled

EXPLANATION OF PLATE XI

Nusselts number (hH/k) versus s/V for a pulsating air jet impinging perpendicularly upon a heated disk from data of Table II.

$R_e = 2 \times 10^3 \pm 3$ percent

$H/d = 15.2$

$d/V = 6.04 \times 10^{-4} \pm 2$ percent

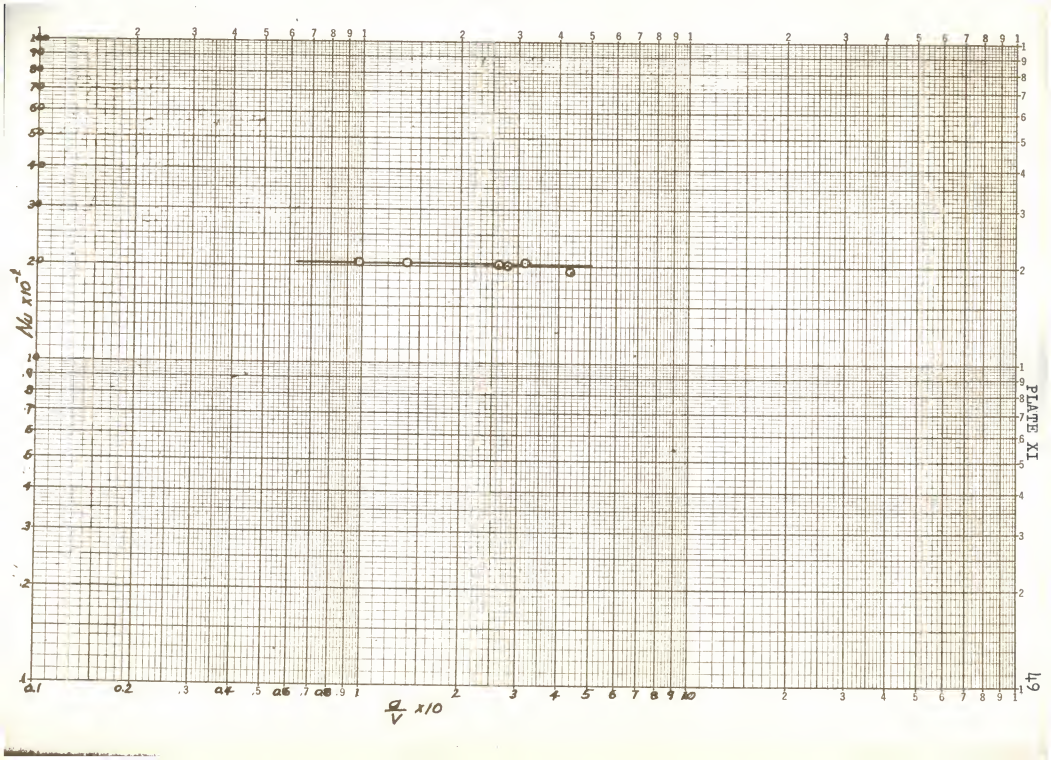

PLATE XI

TABLE II

Pulsation amplitude ft/sec.	Pulsation frequency cps	Nozzle elevation in.	Nozzle diameter in.	Mean Nozzle velocity ft/sec.	Wattmeter reading watts	Jet temp. °F	Disk average temp. °F	Guard ring minus disk rim temperature °F
10.6	2	1.5	0.125	40.7	106.2	88	230.9	0
11.6	2	1.5	0.125	41.6	105.3	90	232.2	-0.13
12.7	2	1.5	0.125	40.4	103.5	94	231	-0.23
4.07	2	1.5	0.125	41.9	105.5	92	233.1	-0.53
5.87	2	1.5	0.125	42.4	105.3	92	233	-0.07

15.16, a/V equalled 0.417, and Reynolds number equalled 1.865×10^3. Table III presents the data taken and Plate XII shows the plot of Nusselts number versus $\omega d/V$ by which the correlation was accomplished. No dependence of Nusselts number upon d/V was found for the range of variables tested which was $\omega d/V = 3.2 \times 10^{-4}$ to 57.5×10^{-4}. This was in spite of claims of the numerous references cited in the introduction. It is possible that a certain critical pulsation frequency must be achieved for there to be any effect of pulsation on the film coefficient. The abrupt drop in Nusselts number at the value of $\omega d/V = 44 \times 10^{-4}$ lends credence to this possibility.

Influence of Prandtls Number

Only air was used for this investigation so that the effect of a varying Prandtl number could not be determined. For this reason the exponent of Prandtls number is assumed to be 0.33 as used by other investigators such as Perry (14) and the researchers mentioned in his paper.

Maximum Radial Wall Jet Velocity Variation Along the Plane Surface

It was pointed out in the analysis that the maximum velocity of the radial wall jet varies as the jet impinges and then flows radially outward. To facilitate solution of the derived differential equations, the manner of variation was experimentally investigated.

EXPLANATION OF PLATE XII

Nusselts number (hH/k) versus $\omega d/V$ for a pulsating air jet impinging perpendicularly upon a heated disk from data of Table III.

$R_e = 1.870 \times 10^3 \pm 1$ percent

$a/V = 0.417$

$H/d = 15.2$

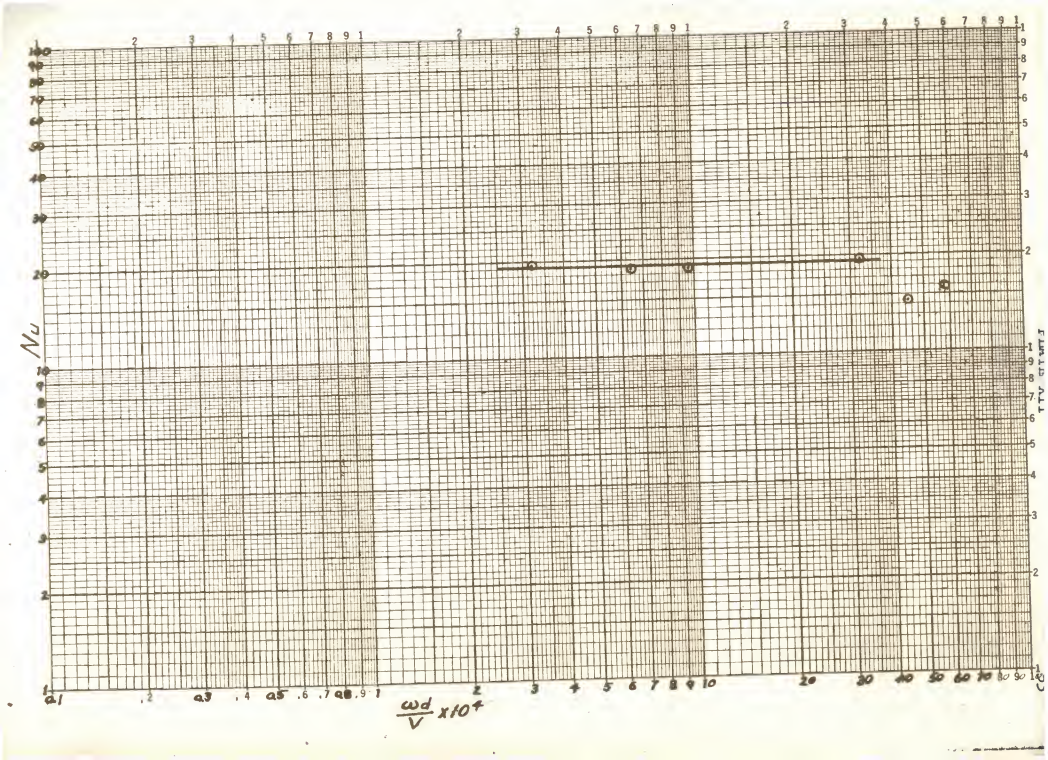
Nu
$\frac{\omega d}{V} \times 10^4$

TABLE III

Pulsation amplitude ft/sec.	Pulsation frequency cps	Nozzle elevation in.	Nozzle diameter in.	Mean Nozzle velocity ft/sec.	Wattmeter reading watts	Jet temp. ^{o}F	Disk average temp. ^{o}F	Guard ring minus disk rim temperature ^{o}F
16.3	18	1.5	0.125	39.1	88.5	91.5	240.2	0
16.3	14	1.5	0.125	39.1	81.9	92.5	242	0.2
16.3	10	1.5	0.125	39.1	98.1	93	230.1	-0.13
16.3	3	1.5	0.125	39.1	96	98	235.5	0.7
16.3	2	1.5	0.125	39.1	97.5	96	234.9	0.4
16.3	1	1.5	0.125	39.1	101.4	96	236	0.1

The plane surface in this case was a glass mirror two feet in diameter. A one-quarter inch diameter nozzle directed a jet of air perpendicularly upon the mirror center. A hot-wire anemometer held in a stand permitting radial and vertical positioning was moved through the thickness of the jet until the point of maximum velocity at some particular radial position was found. Because of the delicate nature of the actual hot wire, it was not possible to make the velocity traverse from the surface of the mirror upward. Instead, the hot wire probe was gradually lowered by means of its stand. Velocity readings while using the hot-wire anemometer as a constant resistance ratio instrument were taken at short spatial intervals and the maximum velocity was found at the point at which the radial wall jet velocity began to decrease. It is estimated that the closest permissible approach of the hot wire to the mirror surface was 1/64 of an inch. The design of this equipment was not suited for determining the elevation above the plate at which the maximum velocity was found, but inclusion of such a feature in equipment for future experimental investigation is recommended for the reason that this information would provide a check on the analytical determination of the hydrodynamic boundary layer thickness which depends upon the maximum radial wall jet velocity's radial distribution.

Plate XIII gives the resultant variation of ρV_{max} with the data given in Tables IV to IX. It is immediately noticed that in the region of less than one nozzle diameter from the nozzle

centerline $\rho V_{max.}$ increases with the distance from the nozzle centerline. This may be caused by the constant addition of air to the jet stream along the plane surface without a compensating increase in thickness of the radial wall jet. Outside the one nozzle diameter region $\rho V_{max.}$ begins to decrease with radial distance from the nozzle centerline. As evidenced by the curve of Plate XIII the spread of data is too great to draw accurate conclusions, but the slope of the curve seems to decrease with increasing flow rates. The curve for both H/d = 15.41 and H/d = 21.16 indicates that Reynolds numbers at the nozzle in the transition range between laminar and turbulent flow $N_{Re} = 2.10^3$ to 2.2×10^3 yield a much greater negative slope than for higher Reynolds numbers. Possibly this is caused by a large decrease in the percentage of entrained environmental air. There is a transition region between positive and negative slopes of $\rho V_{max.}$ versus r/d which takes place at an r/d ratio dependent upon the H/d ratio. Increasing the H/d ratio increases the r/d ratio at which this transition occurs. Due to the limited data, only trends can be concluded and no detailed expressions are set forth.

EXPLANATION OF PLATE XIII

Maximum radial wall jet velocity variation along a plane surface for a steady air jet impinging perpendicularly and plotted as $\rho V_{max.}$ (lb_m/ft^2 sec.) versus r/d from data of Tables IV to IX.

○, □, △ H/d = 15.4

+, ⏢, ◇ H/d = 21.2

PLATE XIII

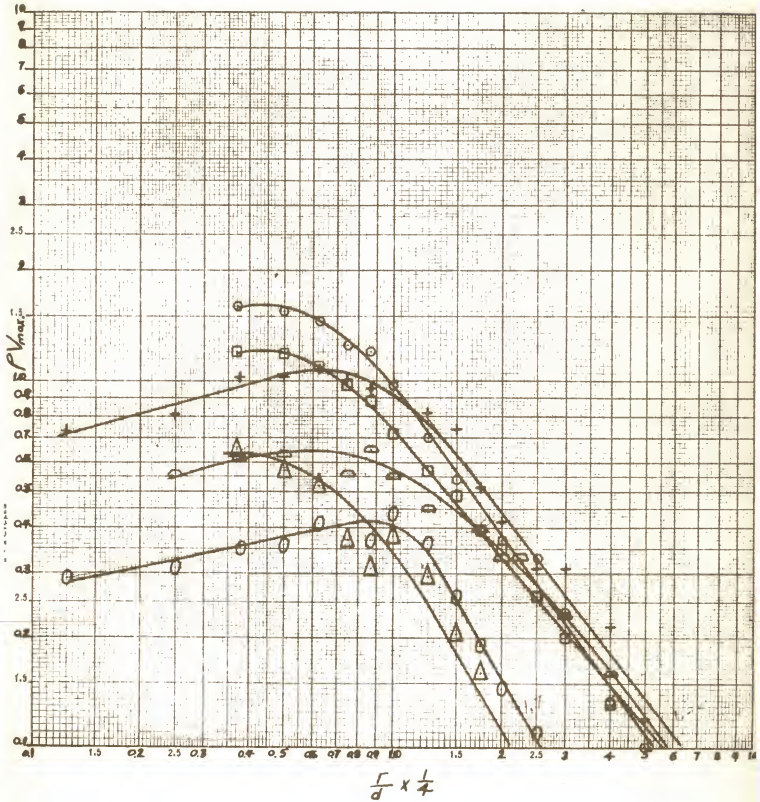

TABLE IV

I x 4 ma	R_r	ρV at Nozzle $lb_m/ft^2 sec.$	Nozzle diameter in.	Nozzle elevation in.	ρV_{max} at radial position $lb_m/ft^2 sec.$	Radial position from center in.
227	1.1	3.72	1/4	4 1/2	1.00	1
223	"	"	"	"	0.837	1 1/4
220.5	"	"	"	"	0.740	1 1/2
214	"	"	"	"	0.537	1 3/4
210	"	"	"	"	0.426	2
205	"	"	"	"	0.314	2 1/2
204	"	"	"	"	0.310	3
200	"	"	"	"	0.219	4
194	"	"	"	"	0.120	5
191	"	"	"	"	0.090	6
190	"	"	"	"	0.0841	7
189	"	"	"	"	0.0729	8
185	"	"	"	"	0.04	10
226	"	"	"	"	0.960	7/8
227	"	"	"	"	1.00	3/4
230	"	"	"	"	1.13	5/8
227.5	"	"	"	"	1.03	1/2
227.5	"	"	"	"	1.03	3/8
222	"	"	"	"	0.81	1/4
220.5	"	"	"	"	0.740	1/8

I = current flowing through the hot wire with anemometer operated as a constant resistance ratio instrument

R_r = resistance ratio

TABLE V

Ixr ma	R_r	PV at Nozzle $lb_m/ft^2 sec.$	Nozzle diameter in.	Nozzle elevation in.	PV_{rad} at radial position $lb_m/ft^2 sec.$	Radial position from center in.
216	1.1	2.16	1/4	4 1/2	0.551	1
212	"	"	"	"	0.449	1 1/4
214	"	"	"	"	0.500	1 1/2
210	"	"	"	"	0.397	1 3/4
207	"	"	"	"	0.325	2
207	"	"	"	"	0.325	2 1/4
201	"	"	"	"	0.212	3
198	"	"	"	"	0.16	4
193	"	"	"	"	0.0961	5
189	"	"	"	"	0.060	6
187	"	"	"	"	0.0462	7
219	"	"	"	"	0.648	7/8
217	"	"	"	"	0.570	3/4
218	"	"	"	"	0.624	1/2
218	"	"	"	"	0.624	3/8
216	"	"	"	"	0.555	1/4

I = current flowing through the hot wire with anemometer operated as a constant resistance ratio instrument.
R_r = resistance ratio.

TABLE VI

I x 4 ma	R_r	PV at Nozzle $lb_m/ft^2 sec.$	Nozzle diameter in.	Nozzle elevation in.	$PV_{max.}$ at radial position $lb_m/ft^2 sec.$	Radial position from center in.
210	1.1	1.41	1/4	4 1/2	0.442	1
207	"	"	"	"	0.367	1 1/4
202	"	"	"	"	0.258	1 1/2
198	"	"	"	"	0.194	1 3/4
196.5	"	"	"	"	0.144	2
192	"	"	"	"	0.110	2 1/2
189	"	"	"	"	0.0713	3
187	"	"	"	"	0.0600	4
184.5	"	"	"	"	0.0441	5
181	"	"	"	"	0.0142	6
207	"	"	"	"	0.367	7/8
208	"	"	"	"	0.386	3/4
209	"	"	"	"	0.401	5/8
206.5	"	"	"	"	0.354	1/2
206	"	"	"	"	0.347	3/8
204.5	"	"	"	"	0.314	1/4
203.5	"	"	"	"	0.292	1/8

I = current flowing through the hot wire with anemometer operated as a constant resistance ratio instrument

R_r = resistance ratio

TABLE VII

I x 4 ma	R_r	PV at Nozzle $lb_m/ft^2 sec.$	Nozzle diameter in.	Nozzle elevation in.	PV_{max} at radial position $lb_m/ft^2 sec.$	Radial position from center in.
209	1.1	1.29	1/4	3 1/16	0.384	1
205	"	"	"	"	0.297	1 1/4
200	"	"	"	"	0.203	1 1/2
197	"	"	"	"	0.16	1 3/4
194	"	"	"	"	0.119	2
194	"	"	"	"	0.119	2 1/2
186	"	"	"	"	0.0420	3
182	"	"	"	"	0.0196	4
180	"	"	"	"	0.0121	5
205.5	"	"	"	"	0.308	7/8
208	"	"	"	"	0.366	3/4
214	"	"	"	"	0.511	5/8
216	"	"	"	"	0.572	1/2
218.5	"	"	"	"	0.648	3/8

I = current flowing through the hot wire with anemometer operated as a constant resistance ratio instrument.
R_r = resistance ratio.

TABLE VIII

I x 4 ma	R_r	ρV at Nozzle $lb_m/ft^2 sec.$	Nozzle diameter in.	Nozzle elevation in.	ρV_{max} at radial position $lb_m/ft^2 sec.$	Radial position from center in.
220	1.1	2.46	1/4	3 1/16	0.714	1
216	"	"	"	"	0.570	1 1/4
213	"	"	"	"	0.493	1 1/2
209	"	"	"	"	0.388	1 3/4
207	"	"	"	"	0.348	2
203	"	"	"	"	0.260	2 1/2
200	"	"	"	"	0.203	3
195	"	"	"	"	0.133	4
192	"	"	"	"	0.0961	5
191	"	"	"	"	0.0870	6
190	"	"	"	"	0.0784	7
225	"	"	"	"	0.893	7/8
227	"	"	"	"	0.976	3/4
230	"	"	"	"	1.10	5/8
232	"	"	"	"	1.19	1/2
232	"	"	"	"	1.19	3/8

I = current flowing through the hot wire with anemometer operated as a constant resistance ratio instrument
R_r = resistance ratio

TABLE IX

I×4 ma	R_r	ρV at Nozzle $lb_m/ft^2 sec.$	Nozzle diameter in.	Nozzle elevation in.	$\rho V_{max.}$ at radial position $lb_m/ft^2 sec.$	Radial position from center in.
227	1.1	36.8	1/4	3 1/16	0.98	1
219	"	"	"	"	0.694	1 1/4
214.5	"	"	"	"	0.537	1 1/2
209	"	"	"	"	0.397	1 3/4
208	"	"	"	"	0.372	2
206	"	"	"	"	0.325	2 1/2
201.5	"	"	"	"	0.235	3
195	"	"	"	"	0.137	4
192	"	"	"	"	0.100	5
195	"	"	"	"	0.137	6
193	"	"	"	"	0.109	7
232	"	"	"	"	1.20	7/8
233	"	"	"	"	1.25	3/4
237	"	"	"	"	1.45	5/8
239	"	"	"	"	1.56	1/2
240	"	"	"	"	1.60	3/8

I = current flowing through the hot wire with anemometer operating as a constant resistance ratio instrument

R_r = resistance ratio

CONCLUSIONS

Experimental data for a pulsating jet of air impinging perpendicularly upon a plane surface shows that the amplitude and frequency of square wave flow rate pulsation do not affect the magnitude of the film coefficient of heat transfer for Reynolds number at the nozzle in the neighborhood of 2×10^3, $\omega d/V = 3.2 \times 10^{-4}$ to 57.5×10^{-4} and $a/V = 7.3 \times 10^{-3}$ to 315×10^{-3}. The range of Reynolds number should be extended to larger values since the possibility exists that an effect of these two variables would then be observed. This is in view of the fact that a Reynolds number of 2×10^3 is in the transition region between laminar and turbulent flow and might be a special case. Due to the limitations of experimental equipment no other pulsation wave form was able to be investigated. Further investigation should be performed at higher values of $\omega d/V$ since the data gives some slight indication that a critical value of this dimensionless group must be attained before the effect of the pulsation frequency is evident. Nusselts number was found to vary with the +0.75 power of H/d and with the 0.66 power of Reynolds number. This result for the dependence of Nusselts upon Reynolds number is in close agreement with Perry (14). No attempt to evaluate the constant coefficient, C, in the dimensional analysis was made since the range of data was not great enough to make such an evaluation of general interest. A dimensionless correlation $N_u = C(N_{Re})^{0.66}(N_{Pr})^{0.33}(H/d)^{0.75}$ is

presented as the result of the experimental work.

Future investigators would do well to work with a polished plane surface to reduce the radiant heat transfer from this surface. Polishing has the advantage of producing a low emissivity compared to an oxidized surface and a resultant low rate of radiant heat transfer. It is felt that proper care in polishing could make this radiant heat transfer less than 1 per cent of the total heat transfer from the surface.

Analytical investigation of the film coefficient of heat transfer for a pulsating jet issuing from a nozzle and impinging upon a plane surface would best be done on a digital computer. The thermal boundary layer which determines the value of the film coefficient depends upon the hydrodynamic boundary layer which is itself difficult to solve. The hydrodynamic boundary layer can possibly be calculated by means of the method of characteristics if a sinusoidal flow rate pulsation is assumed, but this method becomes unbearably complex when the thermal boundary layer is considered. Before programming on the digital computer can be accomplished, further experimental work must be done to determine the time required for a change in flow rate at the nozzle to be propagated to some downstream position. Equipment adequate for such an investigation is described in the section entitled, "Description of Equipment".

This thesis is not presented as a conclusive study of the stated problem. For the most part, trends alone are given. More experimental and analytical work remains to be done before the problem can be said to be fully solved.

ACKNOWLEDGMENTS

The author wishes to express his appreciation for the guidance of Dr. Nevins in the preparation of this thesis and the counsel he gave during the preceding investigation. To Mr. Neely and Mr. Harri the author extends his thanks for their aid in taking experimental data.

BIBLIOGRAPHY

(1) Andreas, A. Ger. 717,766, February 5, 1952 (Cl. 17f. 1203)

(2) Bakke, P. "An Experimental Investigation of a Wall Jet." Journal of Fluid Mechanics, July 1957, 2:467-472.

(3) Bloom, M. H. and M. H. Steiger. "Some Compressibility and Heat Transfer Characteristics of a Wall Jet." Third U. S. National Congress of Applied Mechanics, Proceedings, 717-727, 1958.

(4) Boelter and Martinelli. "The Effect of Vibration on Heat Transfer by Free Convection From A Horizontal Cylinder." New York: Wiley & Sons, 1938. 578-584. Fifth International Congress For Applied Mechanics, Cambridge, Massachusetts.

(5) Eckert and Drake. Heat and Mass Transfer. New York: McGraw-Hill Book Company, 1959. 131-177.

(6) Glauert, M. B. "The Laminar Boundary Layer on Oscillating Plates and Cylinders." Journal of Fluid Mechanics, 1956. 1:97.

(7) _____. "The Wall Jet." Journal of Fluid Mechanics, December 1956, 1:625-643.

(8) Jakob and Hawkins. Elements of Heat Transfer. New York: Wiley & Sons, 1957.

(9) Krzywobloki, M. F. "Fundamentals and Mathematical Theory of Free Boundary Flow and Jets." Jet Propulsion, September 1956, No. 9, 26:760.

(10) Lemlich, R. Ind. Eng. Chem. 47:1175, 1955.

(11) Lighthill, M. J. "The Response of Laminar Skin Friction and Heat Transfer to Fluctuations in the Stream Velocity." Royal Society of London, Proceedings. Series A, 224:1-23. June 1954.

(12) Milne-Thomson, L. M. Theoretical Hydrodynamics. New York: Macmillan and Company, 1938.

(13) Ostrock, Simon. "Note on Aerodynamic Heating of an Oscillating Surface." NACA, Technical Note 3146. April 1954.

(14) Perry, K. P. "Heat Transfer by Convection From a Hot Gas Jet to a Plane Surface." Institution of Mechanical Engineers, Proceedings. 775-780, 1954.

(15) Riley, N. "Effects of Compressibility on a Laminar Wall Jet." Journal of Fluid Mechanics, November 1958, 6:615.

(16) Rommie, F. E. "Heat Transfer to Fluids Flowing with Velocity Pulsations in a Pipe." Unpublished address to Third National Heat Transfer Conference, University of Connecticut, Storrs, Connecticut, August 10, 1959.

(17) Schlichting, Herman. Boundary Layer Theory. New York: McGraw-Hill Book Company, 1955.

(18) Seban, R. A. and D. L. Doughty. "Heat Transfer to Turbulent Boundary-Layers with Variable Free-Stream Velocity." ASME, Semi-Annual Meeting. Paper No. 55-SA-68, 1955.

(19) Sparrow, E. M. and R. Siegel. "Thermal Entrance Region of a Circular Tube Under Transient Heating Conditions." Third U. S. National Congress of Applied Mechanics, Proceedings. 817-826, 1958.

(20) West, F. B. and A. T. Taylor. Chemical Engineering Progress, 1952, 48:39-43.

APPENDICES

APPENDIX I

Assume that h is a function of the variables as indicated,

$h = f(k, \rho, \mu, c_p, \omega, H, D, V, a)$

k = thermal conductivity of the jet fluid, $\frac{Btu}{hr.}\ ^{o}F$ ft.

ρ = mass density of the jet fluid, $lb_m/ft.^3$

μ = dynamic viscosity of the jet fluid, $lb_m/hr.$ ft.

c_p = specific heat of the jet fluid, $Btu/lb_m\ ^{o}F$

ω = oscillation frequency, radians/hr.

H = height of the apparent jet origin above plate, ft.

d = diameter of nozzle, ft.

V = mean jet velocity at nozzle, ft./hr.

h = film coefficient of heat transfer, $Btu/hr.\ ft.^2\ ^{o}F$

a = amplitude of jet velocity oscillation at nozzle, ft./hr.

Choose the dimensions of time (T), length (L), mass (M), and temperature (t), as fundamental dimensions. Express the variables in terms of their dimensions and let θ represent heat

$h = Btu/hr.\ ft.^2\ ^{o}F = \theta/TL^2t$

$k = Btu/hr.\ ft.\ ^{o}F = \theta/TLt$

$\rho = M/L^3$

$\mu = M/LT$

$c_p = \ /Mt$

$\omega = I/T$

$H = L$

$d = L$

$V = L/T$

$a = L/T$

But heat Θ is a form of energy and so can be considered to be equivalent to work. Therefore, since work equals force multiplied by the distance in the direction of the force through which the force acts, it can be said that $\Theta = FL$ where F is the dimension of force.

So, $\Theta = FL = (M)(\text{acceleration})(L) = (M)\ (L/T^2)\ (L)$

and has the dimensions as indicated by $\Theta = ML^2/T^2$.

Rewriting the variables in terms of the fundamental dimensions,

$h = M/T^3t$	$\omega = I/T$
$k = ML/T^3t$	$H = L$
$\rho = M/L^3$	$d = L$
$\mu = M/LT$	$V = L/T$
$c_p = L^2/T^2t$	$a = L/T$

Now, definition of the fundamental dimensions in terms of selected variables can proceed as follows:

$L = d$ $\quad \rho = M/L^3 = M/d^3$ $\quad \rho d^3 = M$ $\quad V = L/T = d/T$ $\quad T = d/V$ $\quad k = M./T^3t = \rho d^3 dv^3/d^3t$ $\quad t = \rho dv^3/k$

Dimensionless π groups may now be formed.

$$\mu = M/LT = \rho d^3 V/dd = \rho dV$$

So, $\pi_1 = \rho dV/\mu$

And $c_p = L^2/T^2t = d^2v^2k/d^2\rho dv^3 = k/\rho dV$

$\pi_2 = \rho dVc_p/k$

Also, $\omega = I/T = V/d$

$\omega d/V = \pi_3$

Similarly, $H = L = d$ $\qquad a = L/T = dV/d = V$

$\pi_4 = H/d$ $\qquad \pi_5 = a/V$

Lastly, $h = M/T^3t = \rho a^3 V^3 K/d^3 \rho dV^3 = k/d$

$\pi_6 = hd/k$

Combining dimensionless groups to obtain conventional dimensionless groups

$\pi_6/\pi_4 = (hd/k)(H/d) = hH/k = N_u$

$\pi_2/\pi_1 = (\rho dV c_p/k)\ (\mu/\rho\, dV) = \mu c_p/k = N_{Pr}$

The remaining dimensionless groups are left as they stand and appear as $\pi_5 = a/V$, $\pi_4 = H/d$, $\pi_3 = \omega d/V$, $\pi_1 = \rho dV/\mu$

Thus, $hH/k = f(\rho dV/\mu\ , \mu c_p/k, \omega d/V,\ H/d,\ a/V)$

Finally, it is assumed that

$hH/k = C(\rho\, dV/\mu)^m\ (\mu\, c_p/k)^n\ (\omega d/V)^o\ (H/d)^p\ (a/V)^q$

where C, m, n, o, p, and q are experimentally determined constants.

APPENDIX II

Apply a momentum balance to the sketched ring shaped differential element.

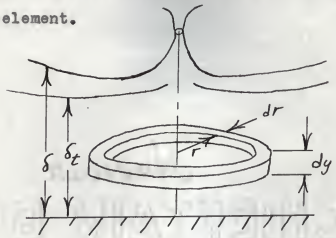

Momentum flux in at r = $2\pi\rho\int_0^{\delta} rU^2 dy$

Momentum flux out at r + dr = $2\pi\rho\int_0^{\delta}(r+dr)(U+\frac{dU}{dr}dr)^2 dy$

Neglecting 2nd order differentials = $2\pi\rho\int_0^{\delta}[rU^2+\frac{d(rU^2)}{dr}dr]dy$

Momentum flux in at δ from continuity requirements $= 2\pi\rho U_e[\int_0^{\delta}(r+dr)(U+\frac{dU}{dr}dr)dy-\int_0^{\delta} rU\,dy]$

$= 2\pi\rho U_e\int_0^{\delta}\frac{d(rU)}{dr}dy\,dr$

where U_e = radial velocity of environmental air.

Momentum flux stored = $2\pi\rho\int_0^{\delta}\frac{d(rU)}{dT}dy\,dr$

Friction force at the plane surface $= -2\pi\mu r\,dr\,\frac{dU}{dy}\Big|_{y=0}$

Pressure force $= -2\pi\delta(r+dr)(P+\frac{dP}{dr}dr)+2\pi r\delta P = 2\pi\delta\frac{d(Pr)}{dr}dr$

Now, $\sum F = \sum Mom._{out} - \sum Mom._{in} + \sum Mom._{stored}$

Substituting from the previous page,

$$-2\pi\mu r\,dr\,\frac{dU}{dy}\Big|_{y=0} - 2\pi\delta\frac{d(Pr)}{dr}dr = 2\pi\rho\int_0^\delta\left[rv^2+\frac{d(rv^2)}{dr}dr\right]dy$$

$$-2\pi\rho\int_0^\delta rv^2\,dy - 2\pi\rho U_e\int_0^\delta\frac{d(rv)}{dr}dy\,dr + 2\pi\rho\int_0^\delta\frac{d(rv)}{dr}dy\,dr$$

Simplifying,

$$\nu r\frac{dU}{dy}\Big|_{y=0} + \frac{\delta}{\rho}\frac{d(Pr)}{dr} = \frac{d}{dr}\int_0^\delta ur(U_e-u)dy - \frac{d}{dr}\int_0^\delta rv\,dy$$

But $U_e = 0 = \frac{d(Pr)}{dr}$. The latter equals zero from Bernoulli's equation which say that the pressure gradient is related to the velocity U_e outside the boundary layer by $\frac{dP}{dx} = -\rho U_e\frac{dU_e}{dx}$

Since $U_e = 0$, $\frac{d(Pr)}{dr} = 0$.

The final form of the hydrodynamic boundary layer equation is then

$$-\nu r\frac{dU}{dy}\Big|_{y=0} = \frac{d}{dr}\int_0^\delta rv^2dy + \frac{d}{dr}\int_0^\delta rv\,dy$$

APPENDIX III

Apply a heat balance to the sketched ring shaped differential element.

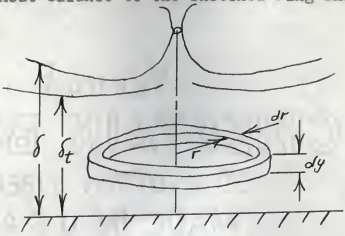

Q carried in at r = $2\pi\rho c_p \int_0^{\delta_t} r v t \, dy$

Q carried out at r + dr = $2\pi\rho c_p \int_0^{\delta_t} (r+dr)(v+\frac{dv}{dr}dr)(t+\frac{dt}{dr}dr)dy$

Neglecting higher order differentials = $2\pi\rho c_p \int_0^{\delta_t} [vt + \frac{d(vt)}{dr}dr]dy$

Q carried in at δ_t from continuity requirements = $2\pi\rho c_p t_e \int_0^{\delta_t} [(r+dr)(v+\frac{dv}{dr}dr) - rv]dy$

and after simplifying = $2\pi\rho c_p t_e \int_0^{\delta_t} \frac{d(rv)}{dr} dy\,dr$

Q conducted in at y = 0 = $-2\pi k r\,dr \frac{dt}{dy}\Big|_{y=0}$

Q stored in element = $2\pi\rho c_p \int_0^{\delta_t} r \frac{dt}{d\tau} dy\,dr$

Now, $\sum Q_{in} = \sum Q_{out} + \sum Q_{stored}$

Substituting from the previous page,

$$2\pi\rho c_p \int_0^{\delta_t} Ut\,dy + 2\pi\rho c_p \int_0^{\delta_t} \frac{d(Urt_e)}{dr}\,dy\,dr - 2\pi k r\,dr \frac{dt}{dy}\Big|_{y=0} =$$

$$2\pi\rho c_p \int_0^{\delta_t} \left[Ut + \frac{d(Urt)}{dr}\,dr\right] dy + 2\pi\rho c_p \int_0^{\delta_t} r \frac{dt}{d\tau}\,dy\,dr$$

Simplifying,

$$-\alpha r \frac{dt}{dy}\Big|_{y=0} = \frac{d}{dr}\int_0^{\delta_t} Ur(t-t_e)\,dy + \frac{d}{d\tau}\int_0^{\delta_t} r\,t\,dy$$

But $t = T - T_e$ so that the above equation becomes

$$-\alpha r \frac{d(T-T_e)}{dy}\Big|_{y=0} = \frac{d}{dr}\int_0^{\delta_t} Ur(T-T_e)\,dy + \frac{d}{d\tau}\int_0^{\delta_t} r(T-T_e)\,dy$$

Again let $U/U_1 = 4\delta\left[2\frac{y}{\delta} - \left(\frac{y}{\delta}\right)^2\right]\left[1 - \frac{y}{\delta}\right]^2$

and $T - T_e / T_{surface} - T_e = \frac{\varphi}{\theta} = \frac{3}{2}\frac{y}{\delta_t} - \frac{1}{2}\left(\frac{y}{\delta_t}\right)^3$

Evaluating integrals, $I = \int_0^{\delta_t} Ur(T-T_e)\,dy = U_1\theta \int_0^{\delta_t} r\frac{U}{U_1}\left(\frac{\varphi}{\theta} - 1\right) dy$

$$I = -\frac{4\delta r}{5} \cdot \frac{U_1\theta}{\delta}\,\delta_t^2$$

$$II = \int_0^{\delta_t} r(T-T_e)\,dy = \theta r \int_0^{\delta_t} \left(\frac{\varphi}{\theta} - 1\right) dy$$

$$II = -\frac{3r}{8}\theta\,\delta_t$$

Also, $$-\alpha r \frac{\partial (T-T_e)}{\partial y}\Big|_{y=0} = -\alpha r \theta \frac{\partial \left(\frac{\theta}{\theta_0}\right)}{\partial y}\Big|_{y=0} = -\frac{3\alpha r \theta}{2\delta_t}$$

The final form of the thermal boundary layer equation is obtained after simplification to be

$$\frac{4\alpha}{\delta_t} = \frac{128}{5r}\frac{\partial}{\partial r}\left(\frac{u r}{\delta}\right)\delta_t^2 + \frac{256}{5}\frac{u_1}{\delta}\delta_t \frac{\partial \delta_t}{\partial r} + \frac{\partial \delta_t}{\partial \tau}$$

HEAT TRANSFER BETWEEN A PLANE SURFACE AND A PULSATING, PERPENDICULARLY IMPINGING AIR JET

by

LOUIS CASIMIR BURMEISTER

B. S., Kansas State University, 1957

AN ABSTRACT OF

A THESIS

submitted in partial fulfillment of the

requirements for the degree

MASTER OF SCIENCE

Department of Mechanical Engineering

KANSAS STATE UNIVERSITY
OF AGRICULTURE AND APPLIED SCIENCE

1959

The heat transfer between a plane surface and a pulsating, impinging jet is investigated both analytically and experimentally. Rather than solve the exact differential equations due to their complexity, first order linear partial differential equations satisfying the same physical laws of conservation of mass, energy, and momentum are derived.

Upon these equations, the hydrodynamic boundary layer thickness (total jet thickness as it flows over the plane surface) and thermal boundary layer thickness depend. Recourse to numerical methods is found necessary for calculation of the film coefficient which determines the magnitude of heat transfer for any particular temperature values. Use of a digital computer to facilitate the many numerical computations is recommended.

A jet of air supplied by a centrifugal fan and issuing from a nozzle impinged perpendicularly upon a copper disk surrounded by a copper annulus with both mounted flush with the surface of a cubic wooden box 2 feet on a side and filled with glass wool insulation served as experimental equipment. Electrical heaters whose output was measured by wattmeters were used. The copper annulus inner circumference was maintained at nearly the same temperature as the outer disk circumference as indicated by thermocouples. Eight copper-constantan thermocouples measured upper surface temperatures of the disk. A solenoid valve with variable flow resistance provided flow pulsation with variable frequency and amplitude by forming a parallel flow path with the nozzle.

Experimental data shows that the amplitude and frequency of square wave flow rate pulsation do not affect the magnitude of the film coefficient of heat transfer for Reynolds number in the neighborhood of 2×10^3, $\omega d/V = 3.2 \times 10^{-4}$ to 57.5×10^{-4} and $a/V = 7.3 \times 10^{-3}$ to 315×10^{-3}. The range of Reynolds number should be extended to larger values since the possibility exists that an effect of these two variables would then be observed. This is in view of the fact that a Reynolds number of 2×10^3 is in the transition region between laminar and turbulent flow and might be a special case. Due to the limitations of experimental equipment, no other pulsation wave form could be investigated. Higher values of $\omega d/V$ should be investigated, since the data gives some slight indication that a critical value of this dimensionless group must be obtained before the effect of the pulsation frequency is evident. A dimensionless correlation $hH/k = C\ (Vd/\nu)^{0.66}\ (H/d)^{0.75}\ (\mu c_p/k)^{0.33}$ where

d = nozzle diameter

H = height of apparent jet origin above disk

V = mean velocity at nozzle

k = thermal conductivity

ν = kinematic viscosity

with all fluid properties determined at the arithmetic average of disk and jet temperature is presented as the result of the experimental work.